Pediatric RESEARCH

www.nature.com/pr

BASIC SCIENCE ARTICLE

LPS-induced maternal inflammation promotes fetal leukocyte recruitment and prenatal organ infiltration in mice

Hannes Hudalla[1,2], Katinka Karenberg[1], Ruben-Jeremias Kuon[3], Johannes Pöschl[1], Raphaela Tschada[1] and David Frommhold[1]

BACKGROUND: A pro-inflammatory intrauterine milieu accounts for increased perinatal morbidity and mortality. We asked how maternal inflammation as seen in endotoxemia affects fetal leukocyte recruitment in vivo during late gestation.

METHODS: Inflammation was induced in pregnant LysEGFP-mice by intraperitoneal LPS injection between gestational day 14 and 18 (E14–E18). After 20 h, intravital fluorescence microscopy was performed on fetal yolk sac venules to examine leukocyte rolling (number of rolling cells/min) and adhesion (>30 s). Infiltration of neutrophils into chorion/amnion, lung, and kidney were quantified by immunofluorescence microscopy.

RESULTS: At high doses (2 × 1 mg/kg), LPS triggered preterm birth (PTB) and intrauterine fetal death (IUFD), with early gestations at high risk of IUFD and late gestations prone to PTB. Lower LPS dosing (2 × 0.25 mg/kg) did not induce labor, but promoted maternal and fetal cytokine production, as well as neutrophilic infiltration of fetal membranes, as seen in chorioamnionitis (CAM). Baseline fetal leukocyte recruitment increased throughout gestation, and maternal inflammation further augmented adhesion at E16–E18. Enhanced leukocyte recruitment ultimately translated into prominent infiltration of fetal lung and kidney.

CONCLUSION: LPS-induced maternal endotoxemia promotes IUFD, PTB, and fetal leukocyte recruitment depending on gestational age. Our proposed model may serve as a platform to test novel perinatal immune modulators.

Pediatric Research (2018) 84:757–764; https://doi.org/10.1038/s41390-018-0030-z

INTRODUCTION

Chronic inflammation and infection remain the leading cause of death in newborns, and especially in premature infants, accounting for a substantial health-burden worldwide.[1] Prenatal exposure to a pro-inflammatory intrauterine milieu is associated with the pathogenesis of preterm labor[2] and severe neonatal complications such as brain injury,[3] necrotizing enterocolitis,[4] and bronchopulmonary dysplasia (BPD).[5] Amniotic infection clinically presents with maternal fever, pain, and signs of endotoxemia.[6] Chorioamnionitis (CAM), the histopathologic correlate of amniotic infection, is marked by mononuclear cell infiltrates into the placenta and fetal membranes.[7] CAM causes dysregulation at the fetomaternal immune interphase by disrupting macrophage phenotype,[8] promoting T_H17 cell activation,[9] and driving the maternal and fetal immune system toward production of T_H1 cell-polarizing cytokines.[10] Combined, these immunological changes can trigger a fetal inflammatory response syndrome (FIRS), translating CAM into a systemic fetal disease with high morbidity.[11,12] In addition to these acute effects, early immune priming by pro-inflammatory stimuli has lasting effects on the development and the immunity throughout childhood.[13] It remains a matter of debate whether it is the fetal or the maternal immune response that mainly contributes to this adverse outcome. Most preclinical models of CAM use intra-amniotic injections of LPS to mimic ascending intrauterine infections by directly activating the fetal innate immune response. However, maternal endotoxemia induced by intraperitoneal (ip) LPS injections has also been shown to induce preterm birth (PTB) and fetal death.[14] Maternal cytokines and pro-inflammatory mediators can pass the placenta and trigger fetal leukocyte activation, recruitment, and organ infiltration.[14,15] Previous studies, however, showed that LPS largely remains within the maternal circulation or does not pass into fetal tissue at all.[14,16] Hence, maternal endotoxemia through LPS injections primarily models the maternal contribution to CAM and adverse fetal outcome. Many pregnant women present with signs of infection are treated with antibiotics for long periods of time to prolong pregnancy. The effect of such inflammation, that does not immediately induce labor, on fetal development and neonatal outcome is incompletely understood.

In this study, we have adapted a proposed model by Sperandio et al. to study fetal leukocyte recruitment on yolk sac (YS) vessels by intravital microscopy (IVM).[17] While acute activation of leukocytes was achieved by fMLP superfusion causing focal-fetal leukocyte rolling and adhesion,[17] the effect of maternal inflammation on fetal leukocyte recruitment has not been described in vivo. Leukocyte recruitment follows a well-described cascade of adhesion molecule-dependent events from the rolling of leukocytes along the inflamed endothelium to firm the adhesion, and eventually the endothelial transmigration,[18–20] and is a key mechanism for the development of FIRS.

The aim of our project was to model the maternal contribution to clinical and histopathological CAM by LPS-induced endotoxemia. At LPS doses that were insufficient to induce preterm labor

[1]Department of Neonatology, Heidelberg University Children's Hospital, 69120 Heidelberg, Germany; [2]Department of Pediatric Newborn Medicine, Brigham and Women's Hospital, Harvard Medical School, Boston, MA, USA and [3]Department of Gynecological Endocrinology and Fertility Disorders, Heidelberg University Hospital, 69120 Heidelberg, Germany

Correspondence: David Frommhold (David.Frommhold@med.uni-heidelberg.de)

These authors contributed equally: Hannes Hudalla, Katinka Karenberg, Raphaela Tschada, David Frommhold.

Received: 14 August 2017 Revised: 3 March 2018 Accepted: 4 April 2018
Published online: 22 August 2018

or death, fetal leukocyte recruitment in vivo and fetal neutrophilic organ infiltration were still heavily promoted by maternal inflammation. We found that this feto-maternal immune cross-talk is ontogenetically regulated. Our novel pre-clinical in vivo model may serve as a platform to study fetal and perinatal immune modulation.

MATERIALS AND METHODS

Animals

LysEGFP reporter mice (C57BL/6N background, EGFP knockin into the neutrophil and monocyte-specific lysozyme M (lys) locus) were used throughout the study.[21] The duration of pregnancy in this mouse strain is 19–20 days. Timed pregnancies were generated by housing a male and two 8–15-week-old females overnight. Animals were separated next morning and vaginal plug-positive mice were classified as E0.5 at noon the same day. All mice were housed in a pathogen-free barrier facility at 22 ± 2 °C, 50–60% humidity, 12/12 h light/dark cycle, and fed with standard mouse chow and sterile water ad libitum. Animals were cared for using guidelines that comply with local regulations for the care and use of laboratory animals. All animal experiments were approved by the Heidelberg University Animal Care and Use Committee and by the Regierungspraesidium Karlsruhe, Baden-Wuerttemberg, Germany (AZ 35-9185.81/G-111/12).

Induction of inflammation

LPS from *E. coli* (LPS 0111:B4, Sigma-Aldrich, Taufkirchen, Germany) was dissolved in saline (10 µg LPS/50 µl). We first titrated LPS-dosing (data not shown) and found that 1 mg/kg LPS injected 20 and 4 h prior to the endpoint did not cause any maternal losses, while still inducing relevant fetal death and PTB. Further titration revealed that 0.25 mg/kg LPS injected 20 and 4 h prior to IVM caused robust fetal leukocyte recruitment without promoting fetal death or PTB. Splitting LPS into two injections reduced fetal death and further allowed for both the analysis of fetal organ infiltration (20 h after the first injection) and acute leukocyte recruitment (4 h after the second injection), as previously established in other in vivo models.[22] Pregnant mice were monitored with a digital camera to record potential PTB, number of pups, and their viability. IUFD or stillbirth was defined as either death upon delivery (no movement) or intrauterine death assessed at the endpoint by a lack of fetal vascular flow on YS vessels by IVM. Control animals were injected with equivalent volumes of saline.

Surgical preparation

Surgical preparation and IVM were performed, as described previously.[17,20] In brief, mice were anaesthetized by ip injection of ketamine (125 mg/kg, KetanestS, Pfizer Pharma GmbH, Berlin) and xylazine (12.5 mg/kg, Xylavet, CP-Pharma GmbH, Burgdorf). Mice were then placed on a heating mat, the trachea was dissected, and a sub-laryngeal tracheal cannula was placed and held in place with sutures. The carotid artery was catheterized for anesthetic maintenance throughout the experiment. A small abdominal incision was performed along the linea alba, and a uterus horn was presented. After careful incision of the uterine wall opposite to the placenta, an individual fetus with intact YS was bedded on viscose gel on a microscope stage and superfused with 37 °C bicarbonate-buffered saline solution. A glass coverslip was placed on the YS and the fetus was submersed in Ringer's solution.

Intravital microscopy

IVM was conducted with an upright microscope (LaVision BioTec GmbH, Bielefeld, Germany, and Olympus BX51W1, Hamburg, Germany) equipped with a 20× universal plan-fluorit objective (UMPLFL20XW/0.50 U M Plan Fluorit, Zeiss) for up to 2 h per mouse on postcapillary venules, as previously described.[17] Rolling of EGFP-labeled cells was assessed as rolling flux (rolling cells/min) and rolling flux fraction (RFF) (rolling cells/total number of labeled cells passing the vessel within 1 min). Adhesion was quantified as the number of (>30 s) adherent cells per square millimeter of vascular surface area.[23] The magnitude of changes in adhesion and rolling between saline-injected and LPS-injected animals were expressed as mean differences (Δmean) or fold change from baseline. All scenes were recorded using a CCD camera (LaVision Imager Compact QE) for later analysis. Vessel diameter, segment length, blood flow velocity, and wall shear rate were measured, as previously described.[24,25]

Systemic leukocyte count

Fetal blood from decapitated fetuses (10 µl) was collected to determine the systemic leukocyte count by staining with Türk's solution (90 µl) (Merck, Germany) under a light microscope.

Histology

To investigate neutrophil infiltration into chorioamniotic membranes and fetal organs, we performed fluorescent microscopy. Fetal organs (lung and kidney), as well as whole-placentas were fixed overnight in 4% paraformaldehyde, dehydrated into ethanol, embedded in paraffin, and sectioned (3 µm). Placentas were cut in a way that the cross-sections displayed all layers from chorioamniotic membranes to the basal plate. The paraffin-embedded tissue sections were rehydrated, permeabilized, blocked, stained with purified rat anti-mouse ly6G antibody (551459, BD Pharmingen), and counterstained with 4′, 6-diamidino-2-phenylindole (DAPI; Sigma-Aldrich Chemie, Schnelldorf, Germany). As a secondary antibody, goat anti-rat IgG (H+L) cy5 conjugate (A10525, Invitrogen) was used. The slides were mounted with Fluoromount-G (SouthernBiotech, Birmingham). Digital images of the organ sections were obtained using an upright fluorescence microscope (Olympus Bx41, Hamburg, Germany) with a CCD camera (Olympus U-CMAD3, Hamburg, Germany). A subset of the placental samples was stained with hematoxylin and eosin, and examined by light microscopy.

Cytometric bead array (CBA)

Fetal blood from decapitated fetuses (E17) was collected and pooled per dam. The CBA mouse inflammation kit (BD Biosciences, San Jose) was used to measure the concentrations of TNFα, MCP-1, IL-6, and IFN-γ from plasma of the dams and fetuses, as per the manufacturer's instructions. A BD LSR II flow cytometer and the BD FCAP Array software v 3.0 (BD Biosciences, San Jose) was used.

Organ infiltration

As the morphology of developing organs varies greatly, and to avoid counting intravascular cells, we standardized neutrophil infiltration into the lung and the kidney, relative to the parenchyma surface area. The area of the vessels and the respiratory tract (alveoli and bronchioli) was quantified using ImageJ (1.45r, Wayne Rasband National Institute of Health) and subtracted from the total area to obtain the parenchymal surface. Similarly, vessels and ducti were subtracted in the kidney samples. Parenchymal ly6G+neutrophils were then counted and expressed as number per mm^2 parenchyma. For placental samples, neutrophil infiltration was standardized to chorioamniotic surface area and expressed as number per mm^2.

Statistics

All statistical analyses were performed using Prism 6 (GraphPad, La Jolla). Multigroup comparisons were performed by one-way or two-way ANOVA, as appropriate, followed by post hoc analysis (Tukey's test) for multiple test adjustment. Two-group comparisons were performed by Student's *t*-test. Changes in the rate of PTB after LPS exposure were analyzed by chi-square test for trend.

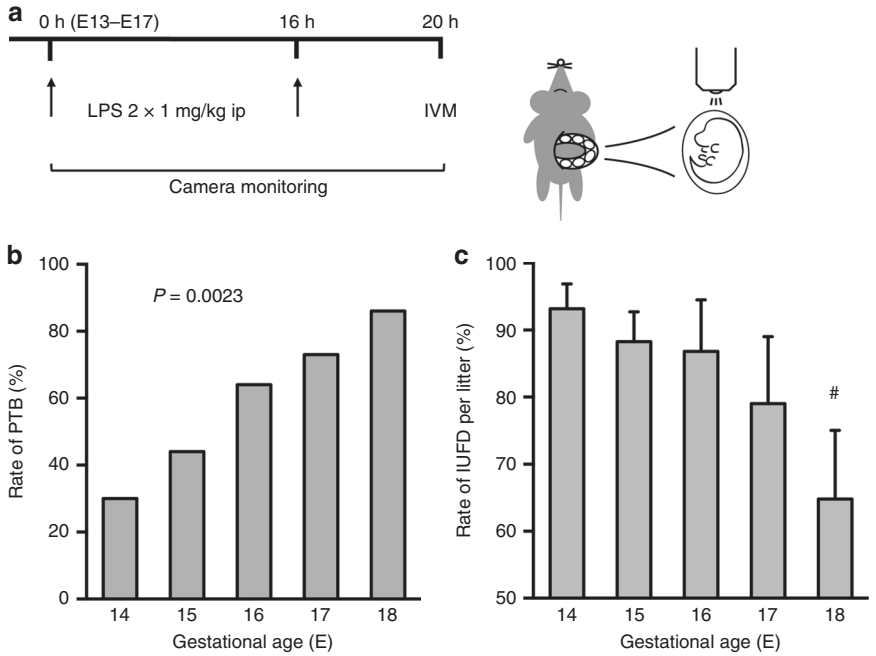

Fig. 1 Rate of preterm birth (PTB) and intrauterine fetal death (IUFD) after maternal LPS injection are gestational age dependent. **a** Experimental timeline and schematic representation of intravital microscopy (IVM). Pregnant mice were injected with 2 × 1 mg/kg LPS ip at E13–E17 20 and 4 h prior to IVM. After LPS injection, mice were monitored with a digital camera. **b** The rate of PTB within the 20 h observation period significantly increased throughout gestation. Statistical analysis by chi-square test for trend ($P = .0023$). **c** The rate of IUFD was defined as stillbirth (monitored by camera) or lack of vascular flow assessed by IVM at endpoint and expressed as mean percentage of total litter + SEM. # represents $P < .05$ compared to E14 by Student's *t*-test. **b**, **c** $n = 9$–14 mice per gestational day, significance was set at $P < .05$

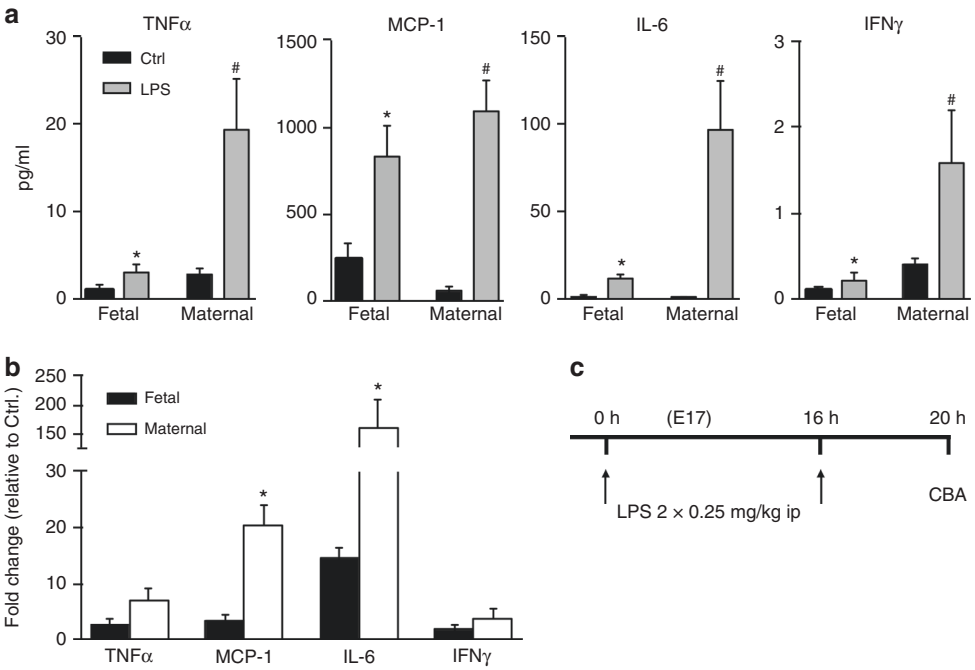

Fig. 2 Maternal LPS-induced endotoxemia causes fetal inflammatory response syndrome (FIRS). Fetal (E17) and maternal blood was sampled after LPS injection, and the pro-inflammatory cytokines TNFα, MCP-1, IL-6, and IFNγ were measured using a CBA kit. **c** Experimental timeline. **a** Cytokines in both fetal and maternal blood are induced after LPS injection. * indicates significant differences to fetal controls, # indicates maternal controls. **b** Fold change in circulating cytokine is significantly higher in maternal blood, compared to fetal blood for MCP-1 and IL-6, indicated by ∗. **a**, **b** Statistical analysis by Student's *t*-test. Data presented as mean + SEM from 7–12 litters for fetal blood and 8–12 pregnant mice per group. Significance was set at $P < .05$

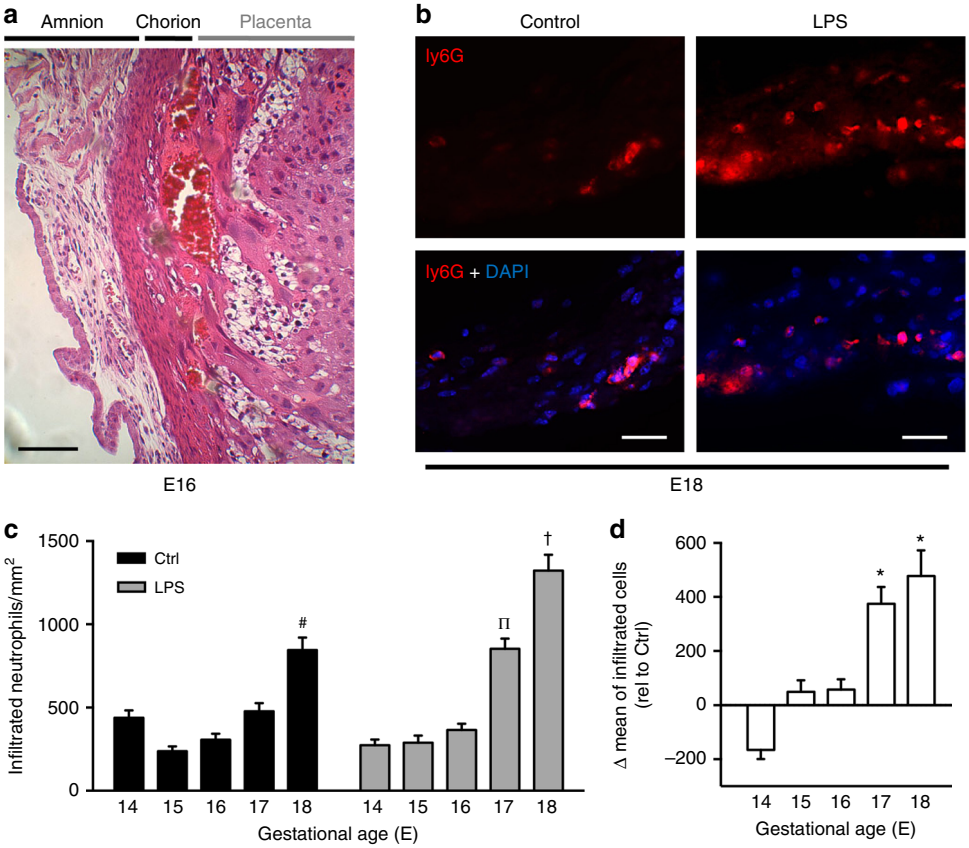

Fig. 3 Maternal LPS exposure triggers chorioamniotic infiltration by neutrophils. Infiltration of neutrophils into chorioamniotic membranes was assessed between E14 and E18 in the absence or presence of maternal LPS-induced inflammation. **a** H&E image of placental cross-section at E16 displaying left to right fetal membranes (black, amniotic membrane (amnion), and chorion) and placenta (gray). **b** Representative immunofluorescence images of chorioamniotic membranes at E18 ± maternal LPS-induced inflammation. Neutrophils were stained with ly6G antibody (cy5, red) and DAPI for nuclear counterstaining (blue). Scale bars are 25 µm. **c** Quantification of neutrophils per mm^2 of chorioamniotic membrane throughout gestation ± maternal LPS-induced inflammation. Statistical analysis by two-way ANOVA and Tukey's post hoc test. Significant differences indicated to E14-17 Ctrl (#), E14-16 LPS (†), and E14-17 LPS (π). **d** Differences in neutrophil infiltration/mm^2 after LPS exposure are displayed as Δmean. Statistical analysis by two-way ANOVA and Tukey's post hoc test. Significant increase of neutrophil infiltration at E17/18 compared to Ctrl (*). **c**, **d** Data presented as mean + SEM from at least three independent litters per group. Significance was set at $P < .05$

Individual tests applied are mentioned in the corresponding figure legends. Statistical significance was set at $P < .05$, values are presented as mean + SEM.

RESULTS

Maternal LPS-induced inflammation and gestation govern the rate of IUFD and PTB

Pregnant mice between E13 and E17 were injected twice with 1 mg/kg LPS ip at 0 and 16 h, and the rate of PTB and IUFD were monitored for 20 h (Fig. 1a). LPS caused an overall high rate of PTB at all ages. However, the rate of PTB further significantly increased from E14 (30%) to E18 (86%) (Fig. 1b). Inversely, the rate of IUFD significantly dropped between E14 and E18 (Fig. 1c). Combined, these data suggest that at a given pro-inflammatory stimulus, early gestation pregnancies (E14) are more prone to IUFD, whereas late gestation pregnancies are more likely to go into preterm labor.

Maternal LPS injection promotes endotoxemia and FIRS

Blood from fetuses at E17 and mothers was analyzed for pro-inflammatory cytokines using a CBA kit (Fig. 2). TNFα, MCP-1, IL-6, and IFNγ were all significantly induced, compared to the control animals, in both fetal and maternal blood (Fig. 2a). The magnitude of fold change upon LPS injection for MCP-1 and IL-6 was significantly higher in maternal blood, compared to fetal blood (Fig. 2b). Interestingly, MCP-1 concentrations were similar between mother and fetus after maternal endotoxemia (Fig. 2b).

Maternal LPS injection triggers neutrophilic infiltration of chorioamniotic membranes

The fetal membranes (chorion and amnion) of placental cross-sections were analyzed 20 h after LPS (2 × 0.25 mg/kg) or saline ip injections (Fig. 3a). The number of ly6G + cells in fetal membranes was quantified by immunofluorescence microscopy and expressed as cells/mm^2 (Fig. 3b). In the absence of LPS, neutrophil counts only significantly increased late in gestation at E18 (Fig. 3c). LPS significantly increased neutrophil infiltration at E17 and E18, compared to control (Fig. 3d). No differences were noted at earlier gestation. To evaluate the effect of LPS on neutrophilic infiltration into fetal membranes independent of underlying ontogenetic changes seen in Fig. 3c, fold difference to baseline were calculated, revealing the largest fold increase in neutrophilic infiltration at E17 (Supplementary Fig. S2a).

Effect of maternal LPS-induced inflammation on fetal leukocyte recruitment in vivo

Adhesion and rolling of EGFP + leukocytes were studied in LysEGFP transgenic mice, that express EGFP under the lysosome M promoter of monomyelocytic cells (neutrophils and monocytes).[21] Leukocyte

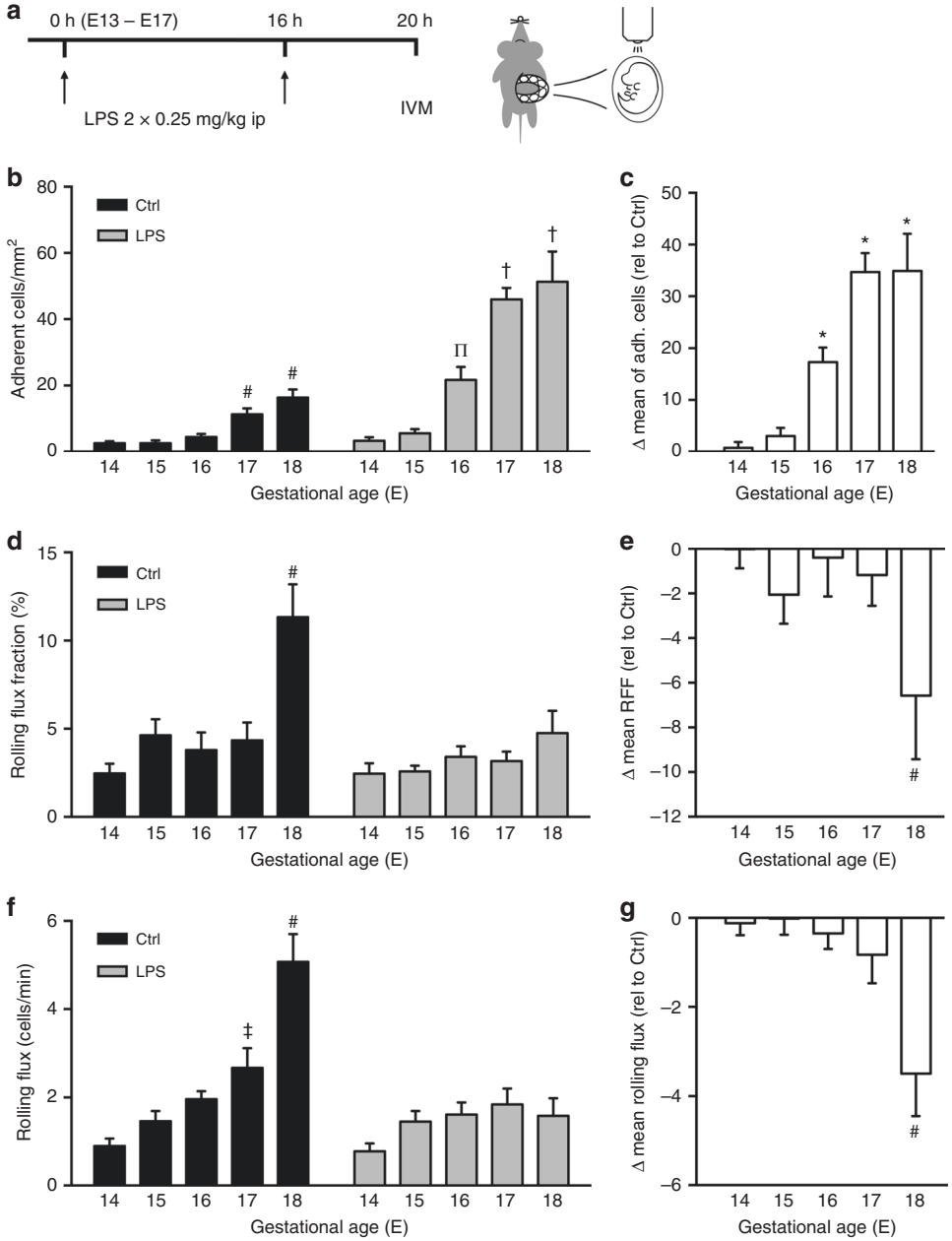

Fig. 4 Maternal LPS exposure modulates fetal leukocyte rolling and adhesion. **a** Experimental timeline: Pregnant mice were injected with 2 × 0.25 mg/kg LPS ip at E13–E17 20 and 4 h prior to IVM. **b** Fetal leukocyte adhesion (number of >30 s adherent cells per mm^2 surface area) was assessed in saline-injected (Ctrl) or LPS-injected mice. Statistical analysis by two-way ANOVA and Tukey's post hoc test. Significant differences are indicated to E14/15/16 Ctrl (#), E14/15/16 LPS (†), and E14/15/17/18 LPS (π). **c** Differences in leukocyte adhesion between Ctrl and LPS are displayed as mean increase (Δmean) upon LPS exposure. Statistical analysis by two-way ANOVA and Tukey's post hoc test. Significant increase of leukocyte adhesion for E16/17/18 after LPS exposure, compared to Ctrl (*). **d** Fetal leukocyte rolling flux fraction (RFF, number of rolling leukocytes per min/total number of labeled cells passing the vessel) was assessed in saline-injected (Ctrl) or LPS-injected mice. Statistical analysis by two-way ANOVA and Tukey's post hoc test. # indicates significant difference to E14/15/16/17 Ctrl. **e** Differences in RFF after LPS exposure are displayed as mean decrease (Δmean). Statistical analysis by two-way ANOVA and Tukey's post hoc test. Significant decrease of leukocyte rolling for E18 after LPS exposure, compared to Ctrl (*). **f** Fetal leukocyte rolling flux (number of rolling leukocytes per min) was assessed in saline-injected (Ctrl) or LPS-injected mice. Statistical analysis by two-way ANOVA and Tukey's post hoc test. Significant differences are indicated to E14/15/16/17 Ctrl (#) and E14/15 Ctrl (‡). **g** Differences in rolling flux after LPS exposure are displayed as mean decrease (Δmean). Statistical analysis by two-way ANOVA and Tukey's post hoc test. Significant decrease of leukocyte rolling for E18 after LPS exposure, compared to Ctrl (*). **b**–**g** All data are presented as mean + SEM. $n = 5$–17 mice per gestational day, significance was set at $P < .05$

recruitment was assessed in saline-injected and LPS-injected (2 × 0.25 mg/kg) pregnant mice between E14 and E18 using IVM in postcapillary YS venules (Fig. 4a), showing similar microvascular and hemodynamic parameters between the two groups (Supplementary Table S1). Fetal leukocyte adhesion (number of >30 s adherent cells per mm^2 vessel surface area) significantly increased throughout gestation in both saline-exposed and LPS-exposed animals (Fig. 4b); however, LPS greatly increased the number of adherent cells, compared to controls, between E16 and E18 (Fig. 4c). In the control group, we found similar trends for leukocyte rolling, with a

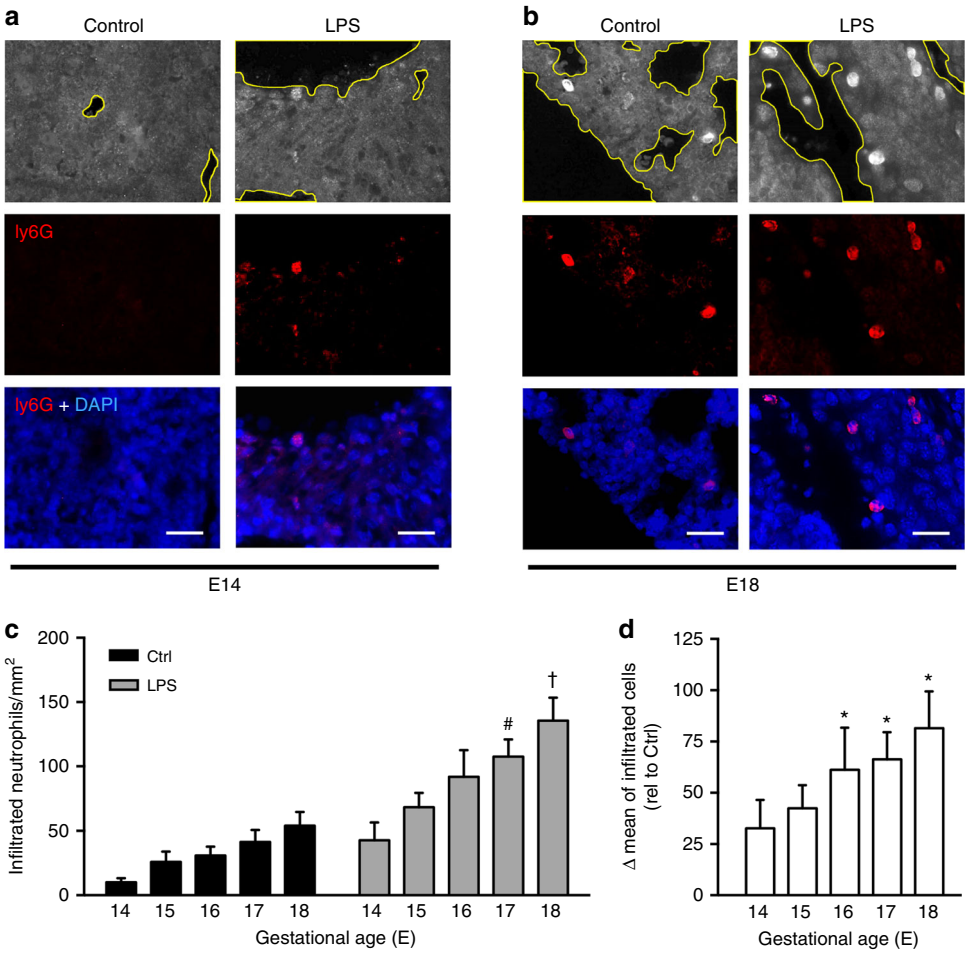

Fig. 5 Maternal LPS exposure triggers neutrophil infiltration of fetal lung. Infiltration of neutrophils into fetal lung was assessed between E14 and E18 in the absence or presence of maternal LPS-induced inflammation. **a** Representative immunofluorescence images of lung tissue at E14. Airway and large vessel surface area were subtracted to calculate the parenchymal lung surface area (first row). Neutrophils were stained with ly6G antibody (cy5, red) and DAPI for nuclear counterstaining (blue) (second row). Only neutrophils outside airways and large vessels were counted for quantification (third row). Scale bars are 25 µm. **b** Representative immunofluorescence images of lung tissue at E18. **c** Quantification of infiltrated neutrophils per mm^2 of lung parenchyma throughout gestation in the absence or presence of maternal LPS-induced inflammation. Statistical analysis by two-way ANOVA and Tukey's post hoc test. Significant differences are indicated to E14 LPS (#) and E14/15 LPS (†). **d** Differences in neutrophil infiltration/mm^2 lung parenchyma after LPS exposure are displayed as Δmean. Statistical analysis by two-way ANOVA and Tukey's post hoc test. Significant increase of neutrophil infiltration at E16/17/18 compared to Ctrl (*). **c**, **d** Data presented as mean + SEM from at least three independent litters per group. Significance was set at $P < .05$

significantly higher RFF (number of rolling leukocytes per min/total number of labeled cells passing the vessel, Fig. 4d) and rolling flux (number of rolling leukocytes per min, Fig. 4f). Contrary to leukocyte adhesion, we saw decreased RFF and rolling flux in the LPS group (Fig. 4d, f), with significant differences at E18 (Fig. 4e, g). To highlight the effect of LPS on leukocyte recruitment independent of underlying ontogenetic changes, we also calculated the fold differences of leukocyte adhesion, RFF, and rolling flux (Supplementary Fig. S1). Fold changes followed a similar pattern of increased adhesion from E16 to E18 (Supplementary Fig. S1a), and significantly decreased rolling at E18 in the LPS-injected group (Supplementary Fig. S1b, c). Example videos of IVM performed are shown in Supplementary Videos S1 and 2.

Maternal LPS exposure triggers neutrophilic infiltration of fetal organs

Infiltration of neutrophils into fetal pulmonary and renal tissue was assessed by histological analysis between E14 and E18 in the absence or presence of maternal LPS-induced inflammation (Figs. 5, 6). The number of ly6G+ cells in fetal parenchyma was determined by immunofluorescence microscopy and expressed as cells/mm^2 (Figs. 5a, b, 6a). Both lung and kidney exhibited similar patterns of neutrophil content with overall comparable counts. Throughout gestation, control animals showed increasing numbers of tissue neutrophils in both lung (Fig. 5c) and kidney (Fig. 6b). However, this increase only reached statistical significance for renal tissue. Exposure to maternal LPS for 20 h greatly increased the neutrophil infiltration in both lung (Fig. 5d) and kidney (Fig. 6c). Interestingly, fold changes of neutrophil infiltration after LPS exposure (compared to control) did not differ significantly between gestational ages for both lung and kidney (Supplementary Fig. S2b, c).

DISCUSSION

CAM is a common condition and is associated with adverse neonatal outcome. CAM is primarily triggered by ascending intrauterine microbial infections; however, the respective contribution of the maternal and fetal immune system to sustain inflammation remains incompletely understood. In

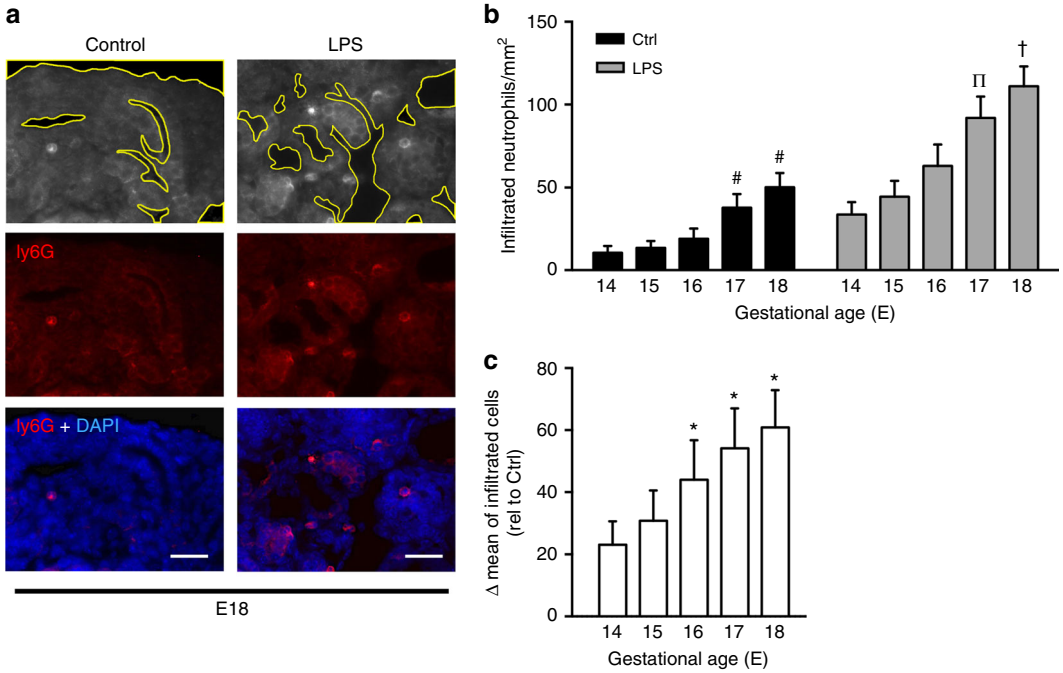

Fig. 6 Maternal LPS exposure triggers neutrophil infiltration into fetal kidney. Infiltration of neutrophils into fetal renal parenchyma was assessed between E14 and E18 in the absence or presence of maternal LPS-induced inflammation. **a** Representative immunofluorescence images of renal tissue at E18. Ducti and large vessel surface area were subtracted to calculate the parenchymal surface area (first row). Neutrophils were stained with ly6G antibody (cy5, red) and DAPI for nuclear counterstaining (blue) (second row). Only neutrophils outside ducti and large vessels were counted for quantification (third row). Scale bars are 25 µm. **b** Quantification of infiltrated neutrophils per mm^2 of renal parenchyma throughout gestation ± LPS-induced inflammation. Statistical analysis by two-way ANOVA and Tukey's post hoc test. Significant differences are indicated to E14/15 Ctrl (#), E14/15 LPS (π), and E14/15/16 LPS (†). **c** Differences in neutrophil infiltration/mm^2 parenchyma after LPS exposure are displayed as Δmean. Statistical analysis by two-way ANOVA and Tukey's post hoc test. Significant increase of neutrophil infiltration at E16/17/18 compared to Ctrl (*). **b**, **c** Data presented as mean + SEM from at least three independent litters per group. Significance was set at $P < .05$

order to delineate maternal and fetal immune contribution, we adapted and combined the previously described models of LPS-induced maternal endotoxemia[14] and fetal in vivo leukocyte recruitment.[17]

Our data suggests that maternal inflammation insufficient to induce delivery or death may still drive relevant infiltration of leukocytes into fetal organs. This has also previously been shown for the infiltration of fetal brain in response to maternal endotoxemia[26,27] and for much lower doses of LPS (1 × 100 µg/kg in pregnant rats or 2.5–50 µg/kg in mice).[28,29] At the same time, our IVM experiments reveal that this effect of maternal inflammation is particularly relevant in late gestation (E16–E18) when leukocytes have matured enough to adequately adhere and extravasate. Our model further shows signs of histological CAM, suggesting that CAM is not only driven by "outside-in" (ascending vaginal infections), but also by "inside-in" (maternal cytokines) inflammation.

Our findings on baseline leukocyte rolling and adhesion closely resemble the previously described ontogenetic changes in murine leukocyte recruitment in vivo, assessed by IVM.[17] The inversely proportional effect of leukocyte adhesion and rolling can be explained by a reduced pool of circulating leukocytes after strong adhesion and extravasation, which is well described in adult IVM models.[19,22] The variation in leukocyte rolling and adhesion within the same litter was low, suggesting that maternal inflammation has an even effect on fetuses, which makes it a more standardized and robust model, compared to intrauterine LPS injections[26].

We also show that LPS-stimulated fetal leukocyte rolling and adhesion is translated into transmigration in the fetal organs between E16 and E18. The clinical relevance of fetal kidney infiltration, as seen in our model, was shown to reduce nephron numbers in fetal sheep.[30] Neutrophilic lung infiltrates are known to predispose to the later development of BPD.[31] Bäckström et al. found that overexpressing IL-1β lead to significant upregulation of CCL2 and CXCL1 (two major neutrophil chemoattractants), and subsequent lung infiltration by neutrophils, leading to the development of BPD only in late gestation. Others similarly describe an impaired fetal capacity to produce cytokine before E16.[14] Combined, these findings suggest that a relevant inflammatory response of the cellular innate immunity only seems to develop as late as E16 to E17. Interspecies comparisons need to be drawn with caution; however, evidence from in vitro studies of human preterm leukocytes also suggests that a similar switch in neutrophil maturation occurs around gestational week 30 in humans, which approximately matches the above-described gestational age in mice.[32,33] If timed unfortunately into this fetal window of vulnerability (late preterms), maternal immune contribution, as seen in pregnancies, burdened with clinical CAM might enhance neonatal adverse outcome.[13]

Taken together, our data delineate the effect of maternal inflammatory stimuli and fetal ontogenetic leukocyte development. We propose that it is the interplay of maternal inflammation and fetal developmental stage that governs adverse neonatal outcome in endotoxemia. Late preterm infants might benefit from perinatal immune modulation to shield against maternal inflammation; however, no such modulators are approved to date. Our proposed model might serve as a preclinical platform for experimental intervention studies.

ACKNOWLEDGEMENTS

We are grateful to Melitta Weissinger for excellent technical and experimental assistance.

FUNDING

This work was partially supported by the German Research Foundation (Deutsche Forschungsgemeinschaft, FR3068/4-1 to D.F.).

ADDITIONAL INFORMATION

The online version of this article (https://doi.org/10.1038/s41390-018-0030-z) contains supplementary material, which is available to authorized users.

Competing interests: The authors declare no competing interests.

REFERENCES

1. Howson, C. P., Kinney, M. V. & Lawn, J. E. *Born Too Soon: The Global Action Report on Preterm Birth*. (World Health Organization, Geneva, 2012).
2. Goldenberg, R. L., Culhane, J. F., Iams, J. D. & Romero, R. Epidemiology and causes of preterm birth. *Lancet* **371**, 75–84 (2008).
3. Wu, Y. W. et al. Chorioamnionitis and cerebral palsy in term and near-term infants. *J. Am. Med. Assoc.* **290**, 2677–2684 (2003).
4. Been, J. V., Lievense, S., Zimmermann, L. J. I. & Kramer, B. W. Wolfs TGAM. Chorioamnionitis as a risk factor for necrotizing enterocolitis: a systematic review and meta-analysis. *J. Pediatr.* **162**, 236–242.e2 (2013).
5. Lapcharoensap, W. et al. Hospital variation and risk factors for bronchopulmonary dysplasia in a population-based cohort. *JAMA Pediatr.* **169**, e143676 (2015).
6. Kim, C. J., Romero, R., Chaemsaithong, P. & Kim, J.-S. Chronic inflammation of the placenta: definition, classification, pathogenesis, and clinical significance. *Am. J. Obstet. Gynecol.* **213**, S53–S69 (2015).
7. Andrews, W. W. et al. The Alabama Preterm Birth study: polymorphonuclear and mononuclear cell placental infiltrations, other markers of inflammation, and outcomes in 23- to 32-week preterm newborn infants. *Am. J. Obstet. Gynecol.* **195**, 803–808 (2006).
8. Ben Amara, A. et al. Placental macrophages are impaired in chorioamnionitis, an infectious pathology of the placenta. *J. Immunol.* **191**, 5501–5514 (2013).
9. Ito, M. et al. A role for IL-17 in induction of an inflammation at the fetomaternal interface in preterm labour. *J. Reprod. Immunol.* **84**, 75–85 (2010).
10. Gargano, J. W. et al. Mid-pregnancy circulating cytokine levels, histologic chorioamnionitis and spontaneous preterm birth. *J. Reprod. Immunol.* **79**, 100–110 (2008).
11. Gantert, M. et al. Chorioamnionitis: a multiorgan disease of the fetus? *J. Perinatol.* **30**, S21–S30 (2010).
12. Hofer, N., Kothari, R., Morris, N., Müller, W. & Resch, B. The fetal inflammatory response syndrome is a risk factor for morbidity in preterm neonates. *Am. J. Obstet. Gynecol.* **209**, 542.e1–542.e11 (2013).
13. Levy, O. Innate immunity of the newborn: basic mechanisms and clinical correlates. *Nat. Rev. Immunol.* **7**, 379–390 (2007).
14. Salminen, A. et al. Maternal endotoxin-induced preterm birth in mice: fetal responses in toll-like receptors, collectins, and cytokines. *Pediatr. Res.* **63**, 280–286 (2008).
15. Carpentier, P. A., Dingman, A. L. & Palmer, T. D. Placental TNF-α signaling in illness-induced complications of pregnancy. *Am. J. Pathol.* **178**, 2802–2810 (2011).
16. Ashdown, H. et al. The role of cytokines in mediating effects of prenatal infection on the fetus: implications for schizophrenia. *Mol. Psychiatry* **11**, 47–55 (2006).
17. Sperandio, M. et al. Ontogenetic regulation of leukocyte recruitment in mouse yolk sac vessels. *Blood* **121**, e118–e128 (2013).
18. Vestweber, D. How leukocytes cross the vascular endothelium. *Nat. Rev. Immunol.* **15**, 692–704 (2015).
19. Braach, N. et al. RAGE controls activation and anti-inflammatory signalling of protein C. *PLoS ONE* **9**, e89422 (2014).
20. Frommhold, D. et al. RAGE and ICAM-1 cooperate in mediating leukocyte recruitment during acute inflammation in vivo. *Blood* **116**, 841–849 (2010).
21. Faust, N., Varas, F., Kelly, L. M., Heck, S. & Graf, T. Insertion of enhanced green fluorescent protein into the lysozyme gene creates mice with green fluorescent granulocytes and macrophages. *Blood* **96**, 719–726 (2000).
22. Frommhold, D. et al. Sialyltransferase ST3Gal-IV controls CXCR2-mediated firm leukocyte arrest during inflammation. *J. Exp. Med.* **205**, 1435–1446 (2008).
23. Sperandio, M., Pickard, J., Unnikrishnan, S., Acton, S. T. & Ley, K. Analysis of leukocyte rolling in vivo and in vitro. *Methods Enzymol.* **416**, 346–371 (2006).
24. Pries, A. R. A versatile video image analysis system for microcirculatory research. *Int. J. Microcirc. Clin. Exp.* **7**, 327–345 (1988).
25. Smith, M. L., Long, D. S., Damiano, E. R. & Ley, K. Near-wall micro-PIV reveals a hydrodynamically relevant endothelial surface layer in venules in vivo. *Biophys. J.* **85**, 637–645 (2003).
26. Elovitz, M. A. et al. Intrauterine inflammation, insufficient to induce parturition, still evokes fetal and neonatal brain injury. *Int. J. Dev. Neurosci.* **29**, 663–671 (2011).
27. Burd, I., Brown, A., Gonzalez, J. M., Chai, J. & Elovitz, M. A. A mouse model of term chorioamnionitis: unraveling causes of adverse neurological outcomes. *Reprod. Sci.* **18**, 900–907 (2011).
28. Gayle, D. A. et al. Maternal LPS induces cytokines in the amniotic fluid and corticotropin releasing hormone in the fetal rat brain. *Am. J. Physiol. Regul. Integr. Comp. Physiol.* **286**, R1024–R1029 (2004).
29. Gleditsch, D. D. et al. Maternal inflammation modulates infant immune response patterns to viral lung challenge in a murine model. *Pediatr. Res.* **76**, 33–40 (2014).
30. Galinsky, R., Polglase, G. R., Hooper, S. B., Black, M. J. & Moss, T. J. M. The consequences of chorioamnionitis: preterm birth and effects on development. *J. Pregnancy* **2013**, 1–11 (2013).
31. Willems, C. H. et al. Poractant alfa (Curosurf®) increases phagocytosis of apoptotic neutrophils by alveolar macrophages in vivo. *Respir. Res.* **13**, 17 (2012).
32. Nussbaum, C. et al. Neutrophil and endothelial adhesive function during human fetal ontogeny. *J. Leukoc. Biol.* **93**, 175–184 (2013).
33. Karenberg, K., Hudalla, H. & Frommhold, D. Leukocyte recruitment in preterm and term infants. *Mol. Cell. Pediatr.* **3**, 35 (2016).